Research article

Innate Immunity

17(3) (2011) 302–320

ISSN 1753-4259 (print)
10.1177/1753425910369269

Cortisol is a potent modulator of lipopolysaccharide-induced interferon signaling in macrophages

Anja M. Billing[1,2], Fred Fack[1], Jonathan D. Turner[1,2], Claude P. Muller[1,2]

[1]*Institute of Immunology, CRP-Santé/National Public Health Laboratory, Luxembourg, Grand Duchy of Luxembourg*
[2]*Graduate School of Psychobiology, University of Trier, Trier, Germany*

The effects of cortisol (CORT) on resting and lipopolysaccharide (LPS)-activated monocyte-derived THP-1 macrophages were investigated by proteomics. Forty-seven proteins were found to be modulated, 20 by CORT, 11 by LPS, and 16 by CORT and LPS. Cortisol-sensitive chaperones and cytoskeletal proteins were mostly repressed. HCLS1, MGN, and MX1 were new proteins identified to be under the transcriptional control of this steroid and new CORT-sensitive variants of MX1, SYWC and IFIT3 were found. FKBP51, a known CORT target gene, showed the strongest response to CORT and synergism with LPS. In resting THP-1 macrophages, 18 proteins were modulated by CORT, with 15 being down-regulated. Activation of macrophages by LPS was associated with enhanced expression of immune response and metabolic proteins. In activated macrophages, CORT had a more equilibrated effect and almost all metabolism-related proteins were up-regulated, whereas immune response proteins were mostly down-regulated. The majority of the LPS up-regulated immune response-related proteins are known interferon (IFN) target genes (IFIT3, MX1, SYWC, PSME2) suggesting activation of the IRF3 signaling pathway. They were all suppressed by CORT. This is the first proteomics study to investigate the effects of CORT on activated immune cells.

Keywords: 2-D DIGE, cortisol, MX1, FKBP51, IRF3, LPS

Introduction

Macrophages belong to the innate immune system and play a key role in pathogen defense by phagocytosis, antigen-processing/presentation and activation/modulation of the adaptive immune response. They are also involved in the progression of many diseases such as multiple sclerosis, cancer, cardiovascular disease or sepsis,[1] which has been related to altered signaling of nuclear receptors, *e.g.* the glucocorticoid receptor (GR).[2] As sentinels of the immune system, macrophages are armed with pattern recognition receptors such as Toll-like receptors (TLRs) to detect invading pathogens. Lipopolysaccharide (LPS), the main cell-wall component of Gram-negative bacteria, is recognized by TLR4 and plays an important role in macrophage activation and induction of co-stimulatory molecules such as CD40, CD80 and CD86 critical for initiation of a specific immune response. This is dependent on LPS-induced interferon (IFN)-β secretion.[3] All TLRs, except for TLR3, use the adapter molecule myeloid differentiation primary response gene 88 (MyD88) which culminates mainly in the activation of nuclear factor kappa-light-chain-enhancer of activated B cells (NF-κB). The MyD88-independent signaling of TLR4 leads to interferon regulatory factor (IRF) 3 activation and is mediated by the adaptor TIR-domain-containing adapter-inducing interferon-β (TRIF), only shared by TLR3 and TLR4. Signature of this pathway is the induction of IFN-β, a type I IFN, which binds to IFN-α receptor 1 (IFNAR1) and induces the IFN autocrine feedback loop. Activated IRF3 induces the expression of

Received 30 November 2009; Revised 15 March 2010; Accepted 15 March 2010

Correspondence to: Claude P. Muller, Institute of Immunology, CRP-Santé/National Public Health Laboratory, 20A rue Auguste Lumière, L-1950 Luxembourg, Luxembourg. Tel: +352 490 604 220; Fax: +352 490-686; E-mail: claude.muller@INS.ETAT.LU

IRF7 and interferon-stimulated gene factor 3 (ISGF3), a transcription factor complex composed of STAT1/STAT2 and IRF9, become activated and induce IFN-α and IFN-inducible genes. Among the TLR family, only TLR4 uses both adapter molecules MyD88 and TRIF, activating both NF-κB and IRF3 pathways.

The glucocorticoid cortisol (CORT), as the end product of the hypothalamic–pituitary–adrenal (HPA) axis, is the most important endogenous inhibitor of inflammation. Psychological and physiological stress activates the HPA axis leading to the adrenal secretion of CORT. Synthetic glucocorticoids are widely used as immunosuppressive drugs in autoimmune diseases (systemic lupus erythrematosus, multiple sclerosis, and rheumatoid arthritis), inflammatory diseases (asthma, atopic dermatitis) and after transplantations. Synthetic glucocorticoids and CORT are also given at high doses in endotoxemia, sepsis, and septic shock, but the therapeutic efficiency is controversial. In systemic inflammation, endogenous CORT is not always sufficient to stop inflammation since septic patients with a high CORT level have a poor prognosis. It is thought that CORT resistance is induced and prevents immunosuppression.

Despite the profound effect of CORT on the immune response, only a few large-scale studies have analyzed the immunomodulatory characteristics of CORT. Messenger RNA expression profiling has been performed on peripheral blood mononuclear cells[4] and monocytes and/or macrophages.[5–9] In an earlier proteomic study using two dimensional difference in-gel electrophoresis (2-D DIGE) combined with matrix assisted laser desorption/ionisation time-of-flight (MALDI-TOF) mass spectrometry, we analyzed the effects of CORT on the resting human monocyte cell line THP-1. In the present study we investigated the immunomodulatory effects of CORT in THP-1 monocyte-derived differentiated by phorbol 12-myristate 13-acetate (PMA) into adherent, highly LPS-susceptible THP-1 macrophages. Here, we have used the same proteomic approach, complemented by immunoblotting and *in-silico* pathway analysis. Our data suggest that CORT differentially influences cell metabolism depending on the differentiation stage of a cell. Furthermore, we show that LPS-induced IFN signaling is strongly influenced by CORT. Our data improve the understanding of the molecular function of CORT and its role in the treatment of sepsis.

Materials and Methods

THP-1 macrophages

THP-1 cells were cultured in RPMI 1640 media (Cambrex, Verviers, Belgium) supplemented with 5% fetal calf serum, 2 mM L-glutamine (Cambrex), mercaptoethanol (Cambrex), sodium pyruvate (Cambrex), 100 U/ml penicillin (Cambrex) and 100 μg/ml streptomycin (Sigma-Aldrich, Bornem, Belgium). The PMA-mediated differentiation of THP-1 cells is an established model to study macrophages. We adapted the protocol by Kang[10] and treated THP-1 cells with 200 nM PMA (Sigma-Aldrich) for 20 h. Cells were allowed to recover for 2 d in fresh media prior treatment with either LPS (1 μg/ml; Sigma-Aldrich), hydrocortisone (CORT, 10^{-6} M; Sigma-Aldrich) or both (Fig. 1). Cortisol at 10^{-6} M reflects a high physiological concentration and was described to be effective in THP-1 monocytes leading to reduced pro-inflammatory cytokine production.[11] Protein was extracted from undifferentiated, untreated THP-1 monocytes and PMA-differentiated THP-1 macrophages after 0, 1, 2, 4, 6, 8, 24 and 48 h. Protein of 48 h treated cells was applied to proteomic profiling. Messenger RNA was extracted after 6 and 72 h. All experiments were performed in triplicate. THP-1 monocytes and macrophages were stained with FITC-labeled anti-CD14 and rhodamin-labeled CD11b antibody and analyzed with a Coulter Epics Elite flow cytometer (Beckman Coulter Inc., Miami, FL, USA). Data analysis was performed using the open source software WinMDI (v2.8).

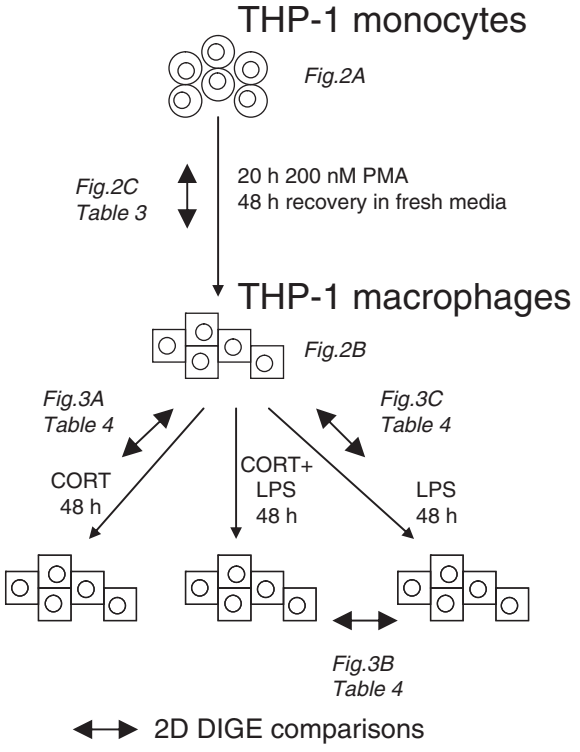

Fig. 1. THP-1 monocyte differentiation into macrophages and treatment with CORT and/or LPS. Double arrows indicate 2-D DIGE comparisons. Reference to the figures and tables are shown in italics.

Sample preparation and CyDye labeling

Total protein of THP-1 cells was extracted by cell lysis using 7 M urea (GE Healthcare, Uppsala, Sweden), 2 M thiourea (GE Healthcare), 4% CHAPS (GE Healthcare), 30 mM Tris (GE Healthcare), 12% isopropanol, a protease inhibitor cocktail (GE Healthcare), and nuclease mix (GE Healthcare; pH 8.5). Nuclear and cytosolic protein was extracted using the Nuclear extract kit (Active Motif Europe, Rixensart, Belgium). Nucleic acids, salts and other impurities were removed by acetone precipitation. Proteins were re-dissolved in cell lysis buffer and quantified using the 2D-Quant Kit (GE Healthcare). For proteomic profiling, samples were fluorescently labeled with Cy2, Cy3 or Cy5 *N*-hydroxysuccinimidyl ester (GE Healthcare; 400 pmol fluorochrome per 50 μg protein). After quenching with 10 mM lysine, the labeled samples were stored at −20°C. Controls and treated samples were labeled randomly with either Cy3 or Cy5. The internal standard, a mix of equal amounts of all samples, was labeled with Cy2. Sample labeling is shown in Table 1.

Two-dimensional gel electrophoresis

For protein electrophoresis, labeled (150 μg total, 50 μg per fluorochrome) and unlabeled protein (200 μg total, 100 μg of each untreated and CORT+LPS treated) was pooled. Sample mixes were loaded on a 24-cm Immobiline™ dry strip, pH 4–7 (GE Healthcare) in a volume of 450 μl rehydration buffer (7 M urea, 2 M thiourea, 30 mM Tris, 4% CHAPS, 1% immobilized pH gradient [IPG] buffer pH 4–7 [GE Healthcare], 200 mM dithiothreithol [DTT; Sigma-Aldrich], traces of bromophenol blue). Isoelectric focusing (IEF) running conditions (I_{max} = 50 μA) were: 300 V for 2 h, followed by linear gradients to 600 V over 3 h, 1 kV over 3 h, 8 kV over 3 h and maintained at 8 kV for 4 h. All IEFs were performed on the Ettan™ IPGphor™ II at 20°C. Subsequently, the IPG-strips were reduced with 0.5% DDT and alkylated by 2.5% iodoacetamide (IAA) in equilibration buffer (50 mM Tris-HCl pH 8.8, 6 M urea, 30% [v/v] glycerol, 2% SDS, and traces of bromophenol blue) for 15 min. Second dimension electrophoresis was performed in 12% SDS-polyacrylamide gels. Gel casting was performed with bind-silane-treated glass plates for automated spot picking.

Fluorescence-labeled proteins were visualized in gel at 100 μm resolution by a Typhoon 9400 fluorescence scanner (GE Healthcare). Image analysis was performed using DeCyder v5.02 (GE Healthcare). In total, nine gels were included in the analysis with biological triplicates for each treatment (Table 1). Separate biological variance analysis (BVA) of four comparisons was performed: THP-1 monocyte-macrophage differentiation (MACRO/MONO), effects of CORT on resting and LPS-activated THP-1 macrophages (CORT/CTRL), CORT+LPS/LPS, and LPS activation (LPS/CTRL). A picking list for one gel of each comparison was generated and processed by the Ettan™ picking robot (GE Healthcare).

Table 1. Sample labeling for 2-D DIGE

Gel no	Experiment	Cy3	Cy5	Cy2
1	1	MONO	MACRO	MIX
2	1	CTRL	CORT	MIX
3	1	LPS	CORT + LPS	MIX
4	2	MACRO	MONO	MIX
5	2	CORT	CTRL	MIX
6	2	CORT + LPS	LPS	MIX
7	3	MONO	MACRO	MIX
8	3	CTRL	CORT	MIX
9	3	LPS	CORT + LPS	MIX

MACRO, THP-1 macrophages; MONO, THP-1 monocytes.

Protein identification by MALDI-TOF MS analysis

Proteins in the picked gel plugs were reduced using 20 mM DTT in 50 mM ammonium bicarbonate (NH_4HCO_3, ABC) for 45 min at 56°C, and subsequently alkylated with 55 mM iodoacetamide in 50 mM ABC for 20 min in the dark. Gel fragments were washed twice with 20 μl 50 mM ABC followed each time by acetonitrile dehydration (10 μl) and residual solvent removed by vacuum centrifugation. Proteins were in-gel-digested with 25 ng trypsin (sequencing grade modified trypsin; Roche) in 25 mM ABC 16 h (37°C). Extracted peptides were dissolved in 0.5 μl of 80% acetonitrile/0.1% trifluoroacetic acid and subsequently mixed with 0.5 μl 2,5 dihydroxybenzoic acid/α-cyano-4-hydroxy-cinnamic acid-matrix mix on a ground target plate (MTP 384 Bruker Daltonics, Leipzig, Germany). Peptide mass fingerprinting (PMF) was performed using a MALDI-TOF/TOF instrument (Ultraflex I, Bruker Daltonics) in the positive reflector mode. Automated spectra acquisition, analysis, internal calibration, baseline subtraction and database search was performed (FlexControl v2.4, FlexAnalysis v2.4, Biotools v3.0, Bruker Daltonics). Search criteria were set to a peptide mass tolerance of 100 ppm and one missing cleavage site. Carbamylmethylation and methionine oxidation were included as possible peptide modifications. Database searches were performed using MASCOT v2.0 (Matrix science, UK) on both the MSDB and Swiss-Prot databases.

Pathway analysis

Pathway Studio® with MedScan technology annotated ResNet Mammalian 6.0 database were used to build networks of differentially expressed proteins in THP-1 monocytes and/or macrophages after CORT and/or LPS treatment. We performed Sub-Network Enrichment Analysis (sNEA) limited to 10 subnetworks with a cut-off *P*-value of 0.05.

Messenger RNA expression analysis

Total RNA was extracted from 1×10^6 cells (Roche, Mannheim, Germany) and reverse transcribed with Superscript III (Invitrogen, Merelbeke, Belgium) according to standard protocols. Relative PCR quantification was performed in 25 µl reactions containing 20 mM Tris–HCl (pH 8.4), 50 mM KCl, 200 mM desoxynucleotide triphosphate, 2 mM $MgCl_2$ (4 mM for FKBP5), 0.5 µM primer, 1 × concentrated SYBR Green (Cambrex) and 2.5 U Platinum Taq DNA polymerase (Invitrogen). Thermal cycling was performed using an Opticon 2 (MJ Research, Landgraf, The Netherlands). Cycling conditions were: 1 cycle 95°C, 10 min and 40 cycles each at 95°C for 20 s and at primer specific annealing temperatures (T_m°C, see Table 2) for 20 s. Primer sets (Eurogentec, Seraing, Belgium) used are listed in Table 2. Samples were normalized to 18S RNA expression using the $\Delta\Delta$Ct method.[12]

One- and two-dimensional immunoblotting

Proteins for 2-D immunoblots (30 µg) were loaded on a 7-cm IPG strip, pH 4–7 (GE Healthcare), in 7 M urea,

Table 2. List of primers

Protein	Gene	NM number	Primer sequences	T_m (°C)
FKBP51	*FKBP5*	NM_004117	F: AAAAGGCCAAGGAGCACAAC R: TTGAGGAGGGGCCGAGTTC	67
IDO	*INDO*	NM_002164	F: GCGCTGTT GAAATAGCTTC R: TTTGGGTCTTCCCAGAACC	67
SYWC	*WARS*	NM_004184	F: GAAAGGCATTTTCGGCTTCA R: CAGCCTGGATGGCAGGAA	60
MX1	*MX1*	NM_002462	F: CTGTTTACCAGACTCCGACACGA R: CCTGTAATTCACAAAGCCTGGC	56
IFIT3	*IFIT3*	NM_001549	F: GATGGTAACAACGAGGCAGCC R: CAGGCGTAGTTTCCCCAAGTG	59
IFN-β	*IFNb*	NM_002176	F: TCAAGGACAGGATGAACTTTGACA R: TTCCAGCCAGTGCTAGATGAATCT	56
TLR1	*TLR1*	NM_003263	F: TTGTCCCACAACAAGTTGGTGA R: GGTGCTCAACCCCAGAAATTTT	55
TLR2	*TLR2*	NM_003264	F: CAGCCTCTCCAAGGAAGAATCC R: ACCAGAGCCTGGAGGTTCACA	59
TLR4	*TLR4*	NM_138554	F: TACAAAATCCCCGACAACCTCC R: TGGATAAATCCAGCACCTGCAG	64
TLR5	*TLR5*	NM_003268	F: TCAACACCACTGAGAGGCTCCT R: GGTTTCTGAAGGCCTCCTTGTC	55
TLR6	*TLR6*	NM_006068	F: AACTGACCTTCCTGGATGTGGC R: GGAATGGATTGTCCCCTGCTT	59
TLR7	*TLR7*	NM_016562	F: TATTCCCACGAACACCACGAA R: GTTGTTTTTTGACCCCAGTGGA	62
IRF1	*IRF1*	NM_002198	F: CAACCAAATCCCGGGGCTCA R: ATGGCCCAGCTCCGGAACAA	61
IRF3	*IRF3*	NM_001571	F: CGTGGCCTGGGTGAACAAGA R: CCCGGGAACATATGCACCAG	58
IRF5	*IRF5*	NM_002200	F: CCAGTACCCAGGGCTTCAATG R: CGCCTTCGGTGTATTTCCCT	62
IRF9	*IRF9*	NM_006084	F: GGCCAGCCAGGGACTCAGAAAGTA R: TTGAGGGAGTCCTGGAGCACAGAG	60
	18S RNA	NT_113958	F: TGAGAAACGGCTACCACATCCA R: CGCTCCCAAGATCCAACTACGA	60

T_m, annealing temperature; F, forward; R, reverse.

2 M thiourea, 30 mM Tris, 4% CHAPS, 1% IPG buffer pH 4–7 (GE Healthcare), 200 mM DTT (Sigma-Aldrich), traces of bromophenol blue in a total volume of 125 µl and rehydrated for 8 h. Isoelectric focussing was performed on an Ettan™ IPGphor™ II at 20°C. The running conditions were: 20 V for 2 h followed by linear gradients to 300 V over 2 h, to 1 kV over 2 h, to 5 kV over 2 h and maintained at 5 kV for 20 min. Subsequently, strips were reduced and alkylated for 15 min with 0.5% DTT and 2.5% IAA in 5 ml 1× SDS loading buffer (Invitrogen). Proteins (1-D and 2-D) were separated under reducing conditions using NuPAGE 4–12% Bis-Tris Zoom gels (Invitrogen) at 200 V for 45 min and transferred to Hybond-ECL PVDF membranes (GE Healthcare) on a semi-dry blotter Model S (Phase, Lübeck, Germany). All blots were blocked with 3% BSA in Tris-buffered saline (TBS)/TWEEN 20 (0.3%) for 1.5 h. Antibody incubations were performed in TBS for 1.5 h at 20–22°C. Primary antibodies used: rabbit anti-FKBP51 at 1:500 (H-100; Santa Cruz Biotechnology, Santa Cruz, CA, USA), chicken anti-human MX1 at 1:1000 (BacLab, Muttenz, Switzerland), rabbit anti-IRF3 (FL-425; Santa Cruz), rabbit anti-PSer396-IRF3 (07-582; Millipore, Upstate, Temecula, CA, USA). As secondary antibodies goat anti-rabbit IgG Cy3, goat anti-mouse IgG Cy3, goat anti-rabbit IgG Cy5 and goat anti-chicken IgG Cy2 at 1:5000 were used (GE Healthcare). IRF3 signals were detected with HRP goat anti-rabbit IgG at 1:5000 (Pierce, Rockford, IL, USA) using ECLplus kit (GE Healthcare). All blots were scanned at 100 µm resolution by a Typhoon 9400 fluorescence scanner (GE Healthcare) and analyzed with ImageQuant (GE Healthcare).

RESULTS

Differentiation of THP-1 monocytes into macrophages

We have previously reported that, in THP-1 monocytes, only four proteins involved in the immune response were modulated by CORT.[13] To investigate further the immunomodulatory effect of CORT, we differentiated THP-1 monocytes by PMA into adherent LPS-sensitive THP-1 macrophages (Fig. 1). Differentiation was confirmed by flow cytometry which showed the induction of the macrophage-specific markers CD14 and CD11b (Fig. 2A,B). We also analyzed PMA-mediated macrophage differentiation by proteomics using 2-D DIGE (Fig. 2C). In total, 12 proteins were identified with 11 up- and 1 down-regulated (P-value < 0.05; Table 3). The strongest induction was observed for vimentin (7-fold), which was identified from six spots, all of which were up-regulated. Its induction and proteasome-mediated degradation has been described as a signature during THP-1 differentiation.[14] Also, cathepsin D, a known macrophage differentiation marker was up-regulated by PMA treatment.[15] The up-regulation of the adapter molecules 14-3-3 delta/zeta and alpha/beta may influence several signaling transduction pathways via interactions with multiple transcription factors. In conclusion, both flow cytometry and change in protein expression supported the differentiation of THP-1 monocytes into macrophages.

Differential protein expression after treatment with cortisol (CORT) and LPS

Resting and LPS-activated THP-1 macrophages were treated for 48 h with a high physiological concentration

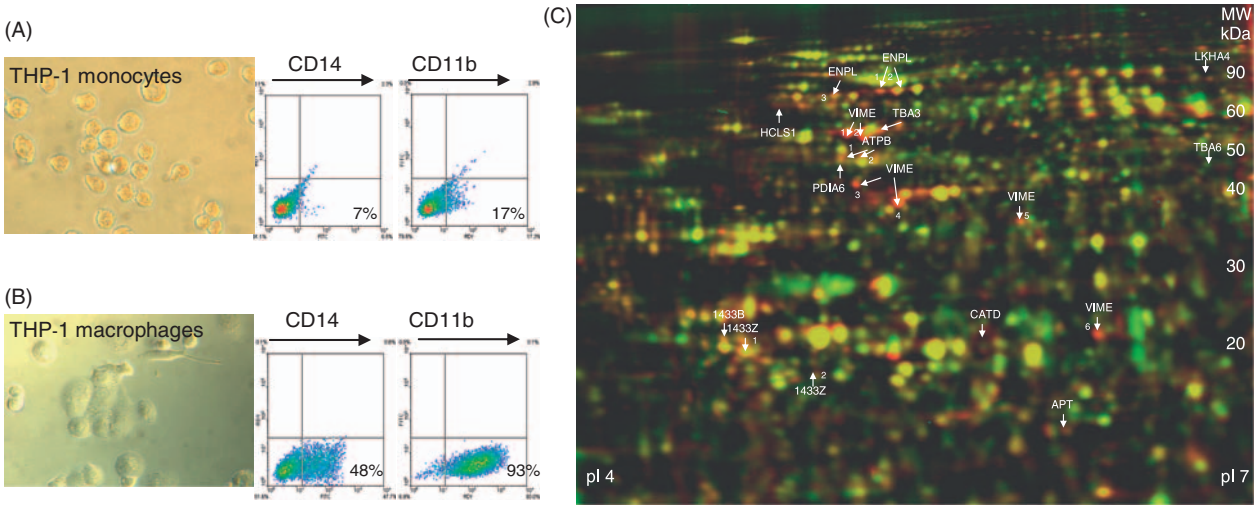

Fig. 2. THP-1 monocyte differentiation into macrophages. (A) THP-1 monocytes and (B) THP-1 macrophages were analysed by light microscopy and flow cytometry for CD14 and CD11b. (C) Representative 2-D DIGE gel (24 cm IPG strip, pH 4–7) of total protein of THP-1 monocytes (Cy3, green) and THP-1 macrophages (Cy5, red).

Table 3. Differential protein expression in THP-1 macrophage differentiation by PMA

Swiss–Prot	(Swiss-Prot accession no.) protein name	MACRO/ MONO	pI	MM (kDa)	SQC (%)	MSC	Expect	MP	Error (ppm)
1433B	(P31946) 14-3-3 protein beta/alpha (protein kinase C inhibitor protein 1) (KCIP-1) (Protein 1054)	1.73	4.76	28.0	46	60	0.016	10	12
1433Z(1)	(P63104) 14-3-3 protein zeta/delta (protein kinase C inhibitor protein 1) (KCIP-1)	2.32	4.73	27.9	44	76	0.00051	11	27
1433Z(2)	(P63104) 14-3-3 protein zeta/delta (protein kinase C inhibitor protein 1) (KCIP-1)	2.06	4.73	27.9	52	102	2^{e}–7	14	30
APT	(P07741) Adenine phosphoribosyltransferase	1.89	5.78	19.6	64	119	2.6^{e}–8	10	44
ATPB(1)	(P06576) ATP synthase beta chain, mitochondrial precursor	2.08	5.26	56.5	29	71	0.00017	10	19
ATPB(2)	(P06576) ATP synthase beta chain, mitochondrial precursor	1.75	5.26	56.5	48	155	6.5^{e}–12	23	13
CATD	(P07339) Cathepsin D precursor	1.48	6.1	45.0	22	61	0.017	8	22
HCLS1	(P14317) Hematopoietic lineage cell-specific protein	1.49	4.74	54.1	22	81	0.00015	8	37
LKHA4	(P09960) Leukotriene A-4 hydrolase	1.92	5.8	69.7	24	56	0.05	11	27
PDIA6	(Q15084) Protein disulfide-isomerase A6 precursor	1.22	4.95	48.5	33	106	5.1^{e}–7	10	10
ENPL(1)	(P13796) Plastin-2 (L-plastin)	1.64	4.7	70.8	29	136	4.1^{e}–10	15	16
ENPL(2)	(P13796) Plastin-2 (L-plastin)	1.96	4.7	70.8	55	286	5.1^{e}–25	29	26
ENPL(3)	(P13796) Plastin-2 (L-plastin)	1.58	4.7	70.8	33	149	2.6^{e}–11	19	29
ENPL(4)	(P13796) Plastin-2 (L-plastin)	2.15	4.7	70.8	29	127	4.1^{e}–9	11	37
TBA1A	(Q71U36) Tubulin alpha-1A chain	2.69	4.94	50.8	48	135	6.5^{e}–10	19	29
TBA1B	(P68363) Tubulin alpha-1B chain	−1.65	4.96	50.5	30	94	7.6^{e}–6	12	21
VIME(1)	(P08670) Vimentin	3.75	5.06	53.5	52	144	1.6^{e}–20	21	25
VIME(2)	(P08670) Vimentin	5.77	5.06	53.5	68	266	5.1^{e}–23	35	29
VIME(3)	(P08670) Vimentin	3.72	5.06	53.5	46	131	2^{e}–9	21	28
VIME(4)	(P08670) Vimentin	7.12	5.06	53.5	26	85	6.2^{e}–5	11	15
VIME(5)	(P08670) Vimentin	2.75	5.06	53.5	24	59	0.024	9	27
VIME(6)	(P08670) Vimentin	4.86	5.06	53.5	32	99	2.5^{e}–6	11	15

Expression changes are given as fold changes (P-value <0.05).
MACRO, THP-1 macrophages; MONO, THP-1 monocytes; pI, isoelectric point; MM, molecular mass; SQC, sequence coverage; MSC, MOWSE score; Expect, reliability of the MS identification; MP, matching peptides.

(10^{-6} M) of CORT and analyzed by 2-D DIGE. Approximately 2500 CyDye-labeled protein spots were resolved per gel. In total, 47 proteins were identified by MALDI-TOF MS that were modulated either by CORT (20), LPS (11) or both (16) using a threshold of >1.5-fold induction/repression (P-value <0.05; Fig. 3). Peptide mass fingerprinting was based on a minimum of five matching peptides with RMS errors ranching from 5 to 55 ppm. HS90B was identified with the highest scores (Mowse score 305; 35 matching peptides; RMS error, 27 ppm) and with a sequence coverage of 47%. The protein SIA8B had the lowest Mowse score (51). It was identified from six peptides with an RMS error of 45 ppm and had a sequence coverage of 26%. Identified proteins were grouped according to their function as chaperones (8), cytoskeletal proteins (9), metabolic proteins (13), immune response-related (9) and transcription/translation-related proteins (8) as shown in Table 4. To simplify, all proteins are named throughout this manuscript according to Swiss–Prot nomenclature. The majority of proteins were identified from single spots; however, some proteins appeared as several spots with different isoelectric point (pI) and molecular mass (MM). FKBP51, SYWC and IFIT3 were observed each as neighboring pairs of spots, probably corresponding to differential phosphorylation levels. SYWC was also observed at 28 kDa truncated at the C-terminus suggesting an alternative transcript or isoform. MX1 was observed at 77, 76 and 45 kDa corresponding to either proteolytic fragments or transcription/splice variants.

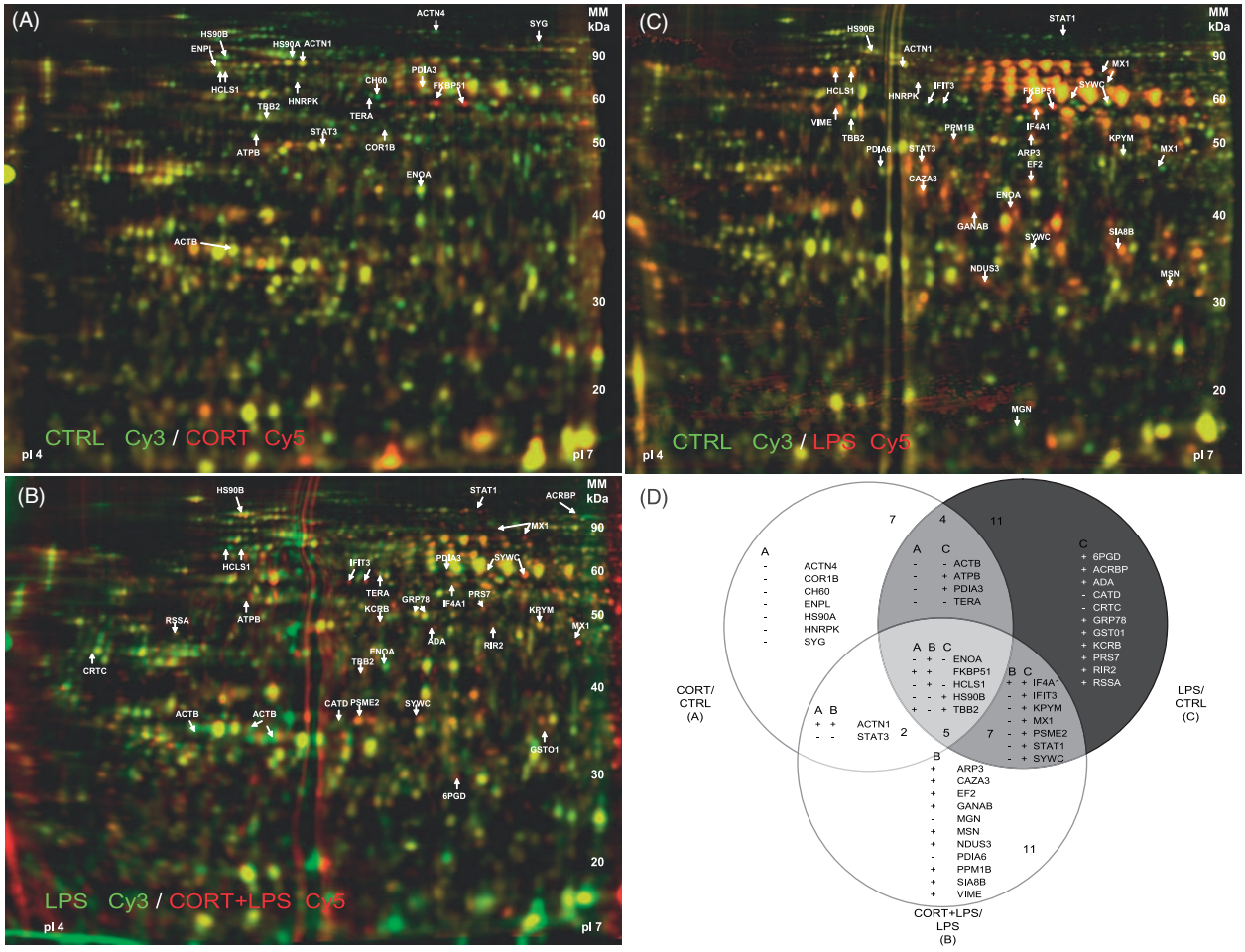

Fig. 3. Cortisol and LPS modulated proteins in THP-1 macrophages. Representative 2-D DIGE gels (24 cm IPG strip, pH 4–7) of total protein of: (A) CTRL (Cy3, green) vs CORT (Cy5, red); (B) LPS (Cy3, green) vs CORT+LPS (Cy5, red); and (C) CTRL (Cy3, green) vs LPS (Cy5, red). The 47 CORT and/or LPS-modulated proteins (threshold 1.5-fold up- or down-regulated, $P < 0.05$) are annotated with the official Swiss–Prot name. (D) Venn diagram shows the three comparisons as three partially overlapping circles: resting THP-1 macrophages with/without CORT (CORT/CTRL); LPS-activated THP-1 macrophages with/without CORT (CORT+LPS/LPS); and THP-1 macrophages versus LPS-activated THP-1 macrophages (LPS/CTRL). Proteins regulated only by CORT are in the open sections, proteins regulated by both CORT and LPS are in light grey sections, proteins regulated only by LPS are in the dark grey sections. Expression status in three column format: CORT/CTRL (A), CORT+LPS/LPS (B), LPS/CTRL (C) with proteins that were either induced (+) or repressed (–) by CORT, and/or LPS.

In resting THP-1 macrophages, 18 proteins were modulated by CORT, with 15 being down-regulated. In activated THP-1 macrophages, CORT had a more balanced effect: 14 proteins were up-regulated while 12 proteins were down-regulated. In activated macrophages, CORT up-regulated all metabolism-related proteins (5 of 5), whereas immune response proteins were mostly down-regulated (6 of 7). In comparison to undifferentiated THP-1 monocytes,[13] 10 proteins were modulated by CORT in both THP-1 monocytes and macrophages (HNRPK, ACTN1, ACTN4, TUBB, CH60, ENPL, FKBP51, HS90A, HS90B, PDIA3), but only three of these were regulated in the same direction (FKBP51↑, HNRPK↓, ACTN1↑).

The strongest CORT-mediated induction (6- and 9-fold) was found for two adjacent FKBP51 spots with identical molecular mass but different pI values. Their expression was further enhanced when LPS was co-administered (6.7- and 12.9-fold). Proteins that were found to be CORT-sensitive were predominantly chaperones (7) and cytoskeletal proteins (9). All chaperones, except FKBP51, were suppressed by CORT.

The activation of macrophages by LPS was associated with enhanced expression of immune response-related proteins (7 of 9) and metabolic proteins (6 of 9; Table 4). In total, 27 proteins were modulated by LPS, 7 of which were repressed and 20 induced. Of these, 11 proteins were only modulated by LPS and were linked to the immune response (2), metabolism (6) and transcription/translation (3), while the other 16 proteins were also regulated by CORT. The latter were classified as cytoskeletal proteins (2), chaperones (2), immune

Table 4. Differential expression of proteins in resting and LPS-activated THP-1 macrophages

Swiss–Prot	(Swiss–Prot accession no.) protein name	THP-1 REST CORT/CTRL[a]	THP-1 ACT LPS+CORT/LPS[b]	THP-1 ACT LPS/CTRL[c]	[d]	pI	MM (kDa)	SQC (%)	MSC	Expect	MP	Error (ppm)
Cytoskeleton												
ACTN1	(P12814) Alpha-actinin-1	1.8	1.97			5.22	14	27	144	1.2[e]–9	27	27
ACTN4	(O43707) Alpha-actinin-4	–1.99				5.27	15	21	145	1.7[e]–10	17	22
ARP3	(P61158) Actin-like protein 3		1.87			5.61	48	35	107	3.5[e]–11	16	17
CAZA3	(Q96KX2) F-Actin capping protein alpha-3 subunit		1.96			7.61	36	21	52	0.01	5	45
COR1B	(Q9BR76) Coronin-1B	–1.54				6.19	55	23	74	0.00011	12	27
MSN	(P26038) Moesin		1.96			9.37	39	55	131	2.4[e]–8	18	31
VIME	(P08670) Vimentin		3.44			5.06	54	18	59	0.019	7	33
ACTB	(P60709) β-Actin	–1.70		–2.22		5.55	43	42	92	8.3[e]–6	15	19
TBB2	(P07437) Tubulin β-2 chain	2	–1.57	2.22		4.82	6	31	106	7.7[e]–6	14	16
Chaperones												
CH60	(P10809) 60 kDa Chaperonin	–1.77				5.7	61	28	104	0.00044	12	22
ENPL	(P14625) 94 kDa Glucose-regulated protein	–2.17				4.7	93	17	66	0.0024	13	16
HS90A	(P07900) Heat shock protein HSP 90-α	–1.84				4.94	85	22	133	6.9[e]–8	14	30
PDIA6	(Q15084) Protein disulfide-isomerase A6 precursor		–1.41			4.95	48	42	191	1.1[e]–15	13	16
FKBP5 (1)	(Q13451) FK506-binding protein 5	6.9	6.73			5.7	52	21	62	0.006	12	13
FKBP5 (2)	(Q13451) FK506-binding protein 5	9.3	12.9			5.7	52	21	62	0.0087	7	11
HS90B	(P08238) Heat shock protein HSP 90-β	–1.98	–1.7	1.64		4.97	83	47	305	3.9[e]–25	35	27
PDIA3	(P30101) Protein disulfide-isomerase A3 precursor	–1.69		2.3		5.98	57	37	130	1.4[e]–9	16	23
GRP78	(P11021) 78 kDa Glucose-regulated protein precursor			1.74		5.07	72	27	104	0.00024	10	21

(continued)

Table 4. Continued

Swiss–Prot	(Swiss–Prot accession no.) protein name	THP-1 REST CORT/CTRL[a]	THP-1 ACT LPS+CORT/LPS[b]	THP-1 ACT LPS/CTRL[c]	[d]	pI	MM (kDa)	SQC (%)	MSC	Expect	MP	Error (ppm)
Immune response												
STAT3	(P40763) Signal transducer and activator of transcription 3	–2.05	–1.54			5.94	89	18	58	0.019	8	48
HCLS1 (1)	(P14317) Hematopoietic cell-specific LYN substrate 1	–1.67	2.1	–1.7		4.74	55	23	59	0.022	8	15
HCLS1 (2)	(P14317) Hematopoietic cell-specific LYN substrate 1		1.92	–2		4.74	55	30	130	3.9[e]–7	13	25
IFIT3 (1)	(O14879) Interferon-induced protein with tetratricopeptide repeats 3		–1.54	4.02		5.12	57	36	125	4.3[e]–9	12	5
IFIT3 (2)	(O14879) Interferon-induced protein with tetratricopeptide repeats 3		–1.86	4.02		5.12	57	21	81	0.0001	11	22
MX1 (1)	(P20591) Interferon-induced GTP-binding protein Mx1			1.9		5.9	76	17	71	0.0072	9	32
MX1(2)	(P20591) Interferon-induced GTP-binding protein Mx1		1.29	3.82		5.9	76	21	92	1.4[e]–5	11	22
MX1(3)	(P20591) Interferon-induced GTP-binding protein Mx1		–2.59			5.9	76	25	80	0.00024	15	18
PSME2	(Q9UL46) Proteasome activator 28-beta subunit		–1.94	2.24		5.44	27	49	107	6.1[e]–6	9	22
STAT1	(P42224) Signal transducer and activator of transcription 1-alpha/beta		–1.48	2.84		5.74	88	19	108	0.006	9	8
SYWC (1)	(P23381) Tryptophanyl-tRNA synthetase			2.35		5.83	53	31	92	9.1[e]–6	10	15
SYWC (2)	(P23381) Tryptophanyl-tRNA synthetase		–2.61	5.72		5.83	53	30	117	3.8[e]–8	13	10
SYWC (3)	(P23381) Tryptophanyl-tRNA synthetase		–1.62	1.95		5.83	53	19	71	0.0011	10	52
CRTC	(P27797) Calreticulin precursor			–1.89		4.3	48	23	59	0.33	6	5
PRS7	(P35998) 26S Protease regulatory subunit 7			3.23		5.72	49	43	163	2.2[e]–8	15	19

Metabolism												
GANAB	(Q14697) Neutral alpha-glucosidase AB precursor		2.14			5.74	17	9	51	0.11	10	17
NDUS3	(O75489) NADH-ubiquinone oxidoreductase 30 kDa subunit		2.44			6.99	30	30	92	0.00018	9	34
PPM1B	(O75688) Protein phosphatase 2C isoform beta		2.82			4.95	53	24	67	0.21	7	45
SIA8B	(Q92186) Alpha-2,8-sialyltransferase 8B		2.16			9.48	43	26	51	0.12	6	45
ATPB	(P06576) ATP synthase beta chain	–1.56		1.58		5.26	57	24	71	3.5^{e}–7	14	15
ENOA	(P06733) Alpha-enolase	–1.56	1.69	–2.29		6.99	47	38	135	9.7^{e}–9	18	16
KPYM	(P14618) Pyruvate kinase isozymes M1/M2		–1.61	1.72		7.95	58	44	216	7.7^{e}–17	23	20
TERA	(P55072) Transitional endoplasmic reticulum ATPase	–1.95		–1.54		5.14	90	24	115	6.3^{e}–6	12	17
6PGD	(P52209) 6-Phosphogluconate dehydrogenase, decarboxylating			1.63		6.88	53	26	103	1.5^{e}–5	9	55
ACRBP	(Q8NEB7) Acrosin-binding protein precursor			1.61		5.09	62	17	46	0.38	4	22
CATD	(P07339) Cathepsin D precursor			–1.82		6.1	45	24	78	0.0051	11	17
GSTO1	(P78417) Glutathione transferase omega-1			1.81		6.23	28	26	50	0.13	8	13
KCRB	(P12277) Creatine kinase B-type			1.58		5.34	43	24	56	0.17	8	20
Transcription/translation												
EF2	(P13639) Elongation factor 2		1.87			6.2	96	15	50	0.12	6	22
HNRPK	(P61978) Heterogeneous nuclear ribonucleoprotein K	–1.6				5.39	51	43	180	6.9^{e}–7	12	36
MGN	(P61326) Protein mago nashi homolog		–2.51			5.74	17	76	122	1.9^{e}–7	10	10
SYG	(P41250) Glycyl-tRNA synthetase	–1.67				6.61	84	12	60	0.0091	10	15
IF4A1	(P60842) Eukaryotic initiation factor 4A-I		2.76	1.67		5.33	46	37	84	6.4^{e}–5	11	32
ADA	(P00813) Adenosine deaminase			3.8		5.63	41	29	110	3.1^{e}–6	13	33
RIR2	(P31350) Ribonucleoside-diphosphate reductase M2 subunit			1.96		5.28	45	22	59	0.085	6	45
RSSA	(P08865) 40S Ribosomal protein SA			–1.59		4.79	33	53	164	1.1^{e}–13	15	21

[a]Effect of cortisol in resting THP-1 macrophages. Comparison: CORT/CTRL.
[b]Effect of cortisol in LPS-activated THP-1 macrophages. Comparison: LPS-activated + CORT/ LPS-activated.
[c]Effect of LPS to activate THP-1 macrophages. Comparison: LPS-activated/CTRL.
[d]Color code for protein modulation: open section-only modulated by cortisol, light grey section- modulated by both cortisol and LPS, dark grey section- only modulated by LPS.
Expression changes are given as fold changes (P-value <0.05), with down-regulated proteins in bold and italic
REST, resting; ACT, LPS activated; pI, isoelectric point; MM, molecular mass; SQC, sequence coverage; MSC, MOWSE score; Expect, reliability of the MS identification; MP, matching peptides.

response (7), metabolism (3) and transcription/translation (1). The LPS-induced immune response-related proteins including SYWC, MX1, IFIT3, STAT1, PSME2, and PRS7 were all except for the latter protein suppressed by CORT.

In our study, several new CORT-regulated proteins were identified including the immune response-related proteins MX1 and HCLS1 and the transcription/translation-related protein magoh-nashi homolog (MGN, *MAGOH*).

Pathway analysis of proteomics data

To establish links and common pathways between the identified proteins, these data together with those from our previous THP-1 monocyte study[13] were submitted for bioinformatic pathway analysis using the data mining software Pathway Studio®. According to the Gene Ontology classification, proteins with a binding capacity for nucleotides, calcium ions, ATP or actin were over-represented among CORT-regulated proteins. The 10 proteins differentially expressed in both THP-1 monocytes and THP-1 macrophages were linked to cell proliferation, apoptosis and mutagenesis (Fig. 4A). Of the 253 GR targets in the ResNet 6.0 database, only HS90A, FKBP51 and ACTB were found to be modulated in this study. Lipopolysaccharide treatment significantly affected the IFN-α pathway in both LPS- and CORT+LPS-treated THP-1 macrophages. In the LPS-treated macrophages, also the IFN-γ pathway was significantly activated. Notably, none of the proteins were directly linked to the NF-κB pathway. Pathway Studio® suggested that ENO1, EF2, VIME, HS90A, STAT1, STAT3, SYWC, MX1, IFIT3 and PSME2 as being part of IFN-α and/or IFN-γ regulated genes (Fig. 4B). Most were up-regulated by LPS and down-regulated by CORT. MX1, a classical type I IFN-inducible protein, is a GTPase that protects the host against a wide range of RNA viruses.[16] It interacts with a variety of calcium channel proteins and may influence their activity. Its implication in the LPS response is not known. The tryptophanyl tRNA synthetase SYWC, the strongest LPS-induced protein, is the only tRNA synthetase that is induced by IFN-γ.[17] Co-expressed with SYWC is the IFN-γ-inducible IDO,[18] which is a highly immunosuppressive tryptophan degrading enzyme, important for the induction of peripheral tolerance by

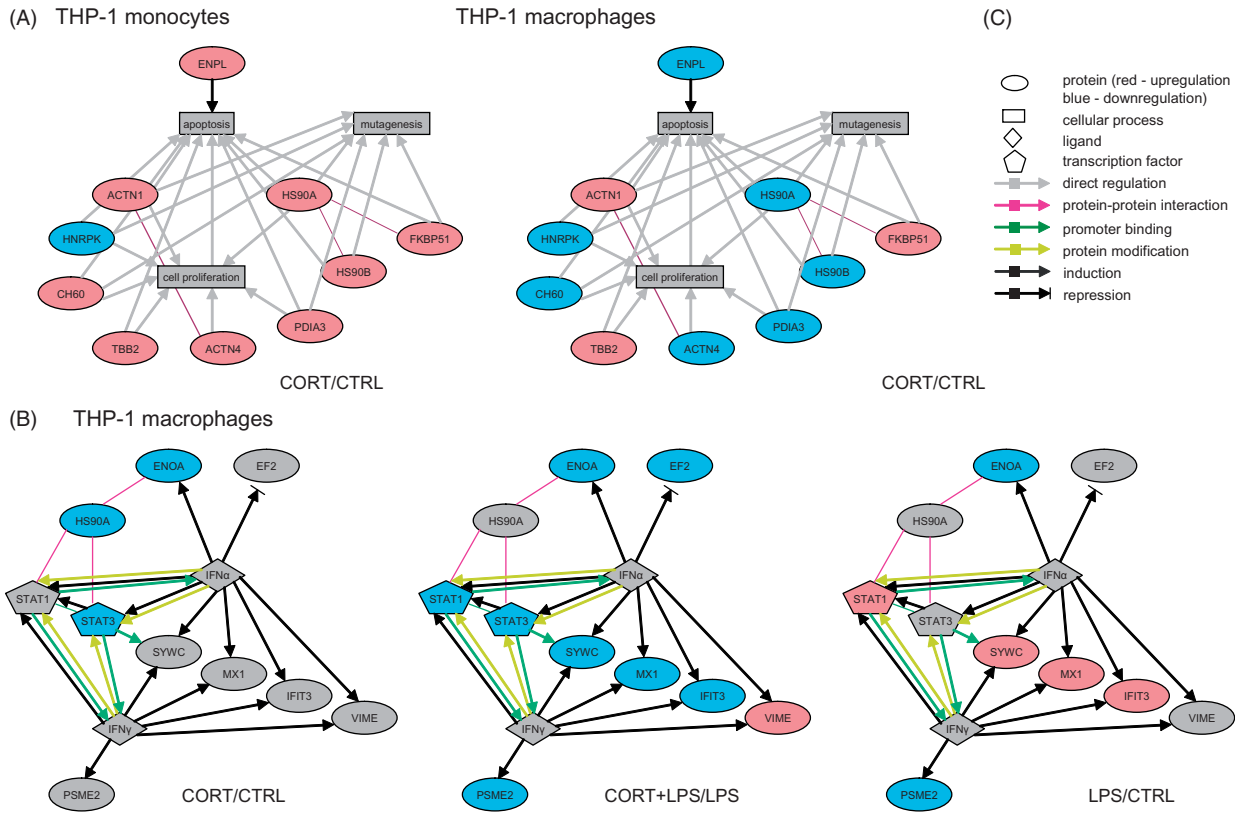

Fig. 4. Pathway analysis using Pathway Studio® 6.0. (A) Overlapping cortisol-modulated proteins in THP-1 monocytes and macrophages were analysed. (B) LPS- and CORT + LPS-treatment in THP-1 macrophages induced IFN-α and IFN-γ signaling pathways. Both pathways were combined and complemented with the up-stream IFN-β and IRF3. Filled objects in blue – down-regulation, in red – up-regulation, in grey – no regulation.

regulatory T-cells, for the prevention of fetal rejection and involved in the development of depression-like symptoms in LPS-treated mice.[19] Two transcription factors of the STAT family, STAT1 and STAT3, were modulated by both CORT and/or LPS. An internally truncated 45-kDa STAT3 isoform was found to be down-regulated by CORT in resting and LPS-activated THP-1 macrophages possibly indicating reduced STAT3 signaling. Signaling of IL-6 and related cytokines induces STAT3 activation leading to homodimerization or heterodimerizion with STAT1. Recently, STAT3 has been found to enhance transcriptional activity of other TFs such as GR.[20] STAT1 homodimers bind to IFN-γ-activated sites (GAS) and induce type II IFN-inducible genes whereas STAT1/STAT2/IRF9 heterotrimers bind to IFN-stimulated response elements (ISRE) and induce type I IFN-inducible genes. Type I IFN-inducible IFIT3 (synonyms: IFIT4, RIG-G) which is mainly expressed in cells with hematopoietic origin, has anti-viral and antiproliferative activity. IFIT3 was identified from two adjacent spots probably representing differentially phosphorylated isoforms containing PSer203 and/or PSer237. Similar to FKBP51, it processes tetratricopeptide repeats mediating the interaction with HS90A. Its induction is STAT1-independent, but can also be induced by IRF1 or IRF9/STAT2.[21] It has been linked to monocyte-differentiation into dendritic cell-like cells.[22] PSME2 (proteasome activator PA28-β) is classically type II IFN inducible and, as part of the immunoproteasome, it is involved in MHC I antigen processing. In mature dendritic cells, its induction was shown to be IFN-γ-independent.[23]

In conclusion, this pathway analysis identified the LPS-activated IFN pathway as a prominent target of immune suppressive activity of CORT.

Effect of CORT and LPS on mRNA expression of IFN-related genes

Lipopolysaccharide acts on the IFN pathway via TLR4, TRIF and IRF3, which is part of the autocrine/paracrine IFN loop. To confirm the suppressive effect of CORT on LPS-activation of IFN-target genes, we measured mRNA expression of some IFN-induced genes (SYWC, IDO, MX1, IFIT3), TLRs and IRFs in THP-1 macrophages. We also included IFN-β as the direct target of IRF3 activation and FKBP51 as a signature of CORT signaling (Fig. 5).

The effect of CORT was confirmed by the induction of FKBP51 after 6 h and remained elevated until 72 h. Co-administration of LPS had no significant effect on the CORT-mediated FKBP51 induction. Interferon-β was rapidly induced (6 h) by LPS and this induction was efficiently suppressed by CORT. Cortisol also suppressed base-line expression of IFN-β. Type I and type II IFN induced genes (MX1, IFIT3 and SYWC, IDO, respectively) were all rapidly (6 h) LPS-induced. Co-administration of CORT suppressed the LPS-mediated induction of SYWC, IDO, and IFIT3. MX1 became suppressed by CORT only after an initial induction. All four IFN-inducible genes were still elevated after 72 h of LPS. Cortisol suppressed this late response at least for SYWC, MX1 and IFIT3. Surprisingly, after 72 h CORT alone induced the expression of IDO, MX1 and IFIT3. This confirms the LPS-mediated induction of type I and type II IFN target genes and their modulation by CORT.

Lipopolysaccharide and IFN alter TLR expression;[24,25] in turn, TLRs modulate the IFN autocrine loop. Therefore, we tested the combined effect of LPS and CORT on TLR expression. Except for TLR7, all investigated TLRs were modulated both by LPS and CORT. After 6 h, CORT alone induced TLR2 and TLR5 and suppressed TLR1. After 72 h, CORT alone had no modulating effect. After 6 h, LPS-induced TLRs 1, 4, 5, 6 and 7, and suppressed after 72 h TLR5 and TLR7. Toll-like receptor 1 remained induced, while TLR4 and TLR6 returned to basal levels. In LPS-activated THP-1 macrophages, CORT induced TLR2 and reduced TLR1 and TLR6. In conclusion, both LPS and CORT modulate the innate sensor system. However, cortisol did not suppress specifically LPS-mediated induction of TLR pathways as was observed for the IFN target genes.

The IRFs are considered to be master regulators of TLR and cytosolic pattern-recognition-receptor signaling. For example, TLR4 signaling is known to affect IRF3 and IRF5.[26] Lipopolysaccharide or CORT had no or little effect on IRF3 or IRF5 expression. A more dramatic effect was observed for IRF1 and IRF9, rapidly (6 h) induced by LPS ($P < 0.001$). Cortisol blunted this induction and accelerated the return to baseline levels. Similar to IFN-inducible genes, CORT stimulated IRF1 and IRF9 after 72 h. Thus, CORT suppresses LPS-induced IRF1 and IRF9 up-regulation.

In conclusion, cortisol is a potent suppressor of the LPS-induced IFN pathway as observed for the IFN target genes probably by reducing IRF expression.

Effect of CORT and LPS on MX1 protein expression

The above 2-D DIGE experiments showed that different isoforms of MX1 were induced by LPS and suppressed by CORT. To confirm further the modulation at a protein level, a series of 1-D immunoblots of MX1 were performed (Fig. 6A). As a control for CORT activity, FKBP51 was included. The IFN response protein MX1 was clearly induced in THP-1 macrophages after 8 h LPS treatment and further increased at least 48 h post-stimulation. The two main MX1 bands corresponded to the 76 kDa and 78 kDa spots on the 2-D gel. The smaller

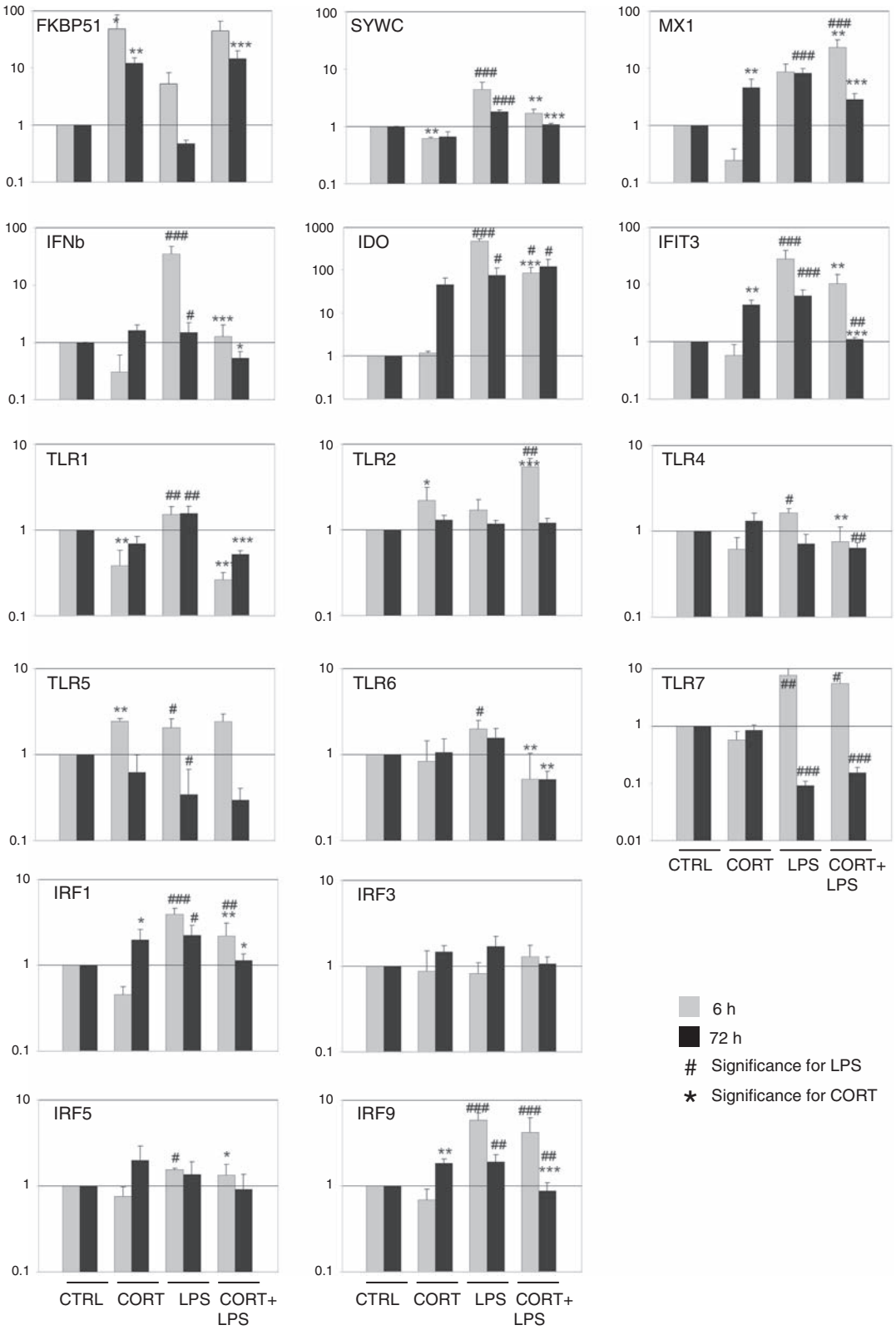

Fig. 5. Gene expression analysis. Messenger RNA expression of CORT-modulated genes (from the proteomics study), TLRs and IRFs in THP-1 macrophages ($n = 3$) after 6 h (grey bars) and 72 h (black bars) of CORT (10^{-6} M) and/or LPS (1 μg/ml) treatment. Expression was related to 18S RNA as a housekeeping gene. Statistical analysis was performed with SigmaStat v3.1 using two-way ANOVA. Multiple comparison procedures have been performed using the Student–Newman–Keuls method. The following comparisons were made for CORT effects: CORT/CTRL and CORT+LPS/LPS, and for LPS effects: LPS/CTRL and CORT+LPS/CORT. Significant effects of CORT (*) and LPS (#) were annotated as: $P < 0.05$ */#, $P < 0.01$ **/##, $P < 0.001$ ***/###. Data are presented as mean ± SD of fold changes (in comparison to control).

MX1 species represented the constitutively expressed MX1 whereas the larger was induced. We confirmed a CORT-mediated suppression of the 78-kDa MX1 by LPS after 48 h (Fig. 6A,B). Further, we investigated the effect of LPS and CORT on the multiple MX1 isoforms by 2-D immunoblotting (Fig. 6C). In untreated THP-1 macrophages, MX1 was present in two groups of spots at 76/77 kDa. The smaller group matched with the theoretical pI of ± 5.6, the other was separated at pI ± 6.3. The small fragment at 45 kDa identified by proteomics was not observed. Under the influence of LPS, two additional groups of spots of distinct sizes (78 kDa and 79 kDa) emerged at pI ± 5.6 containing up to 7 adjacent spots (78 kDa). In the presence of CORT, the MX1 species at pI ± 5.6 were all larger than those at pI ± 6.3. Also, the spot distribution was different under CORT with six spots at 78 kDa and four spots of 77 kDa. Currently, three phosphotyrosines have been described for MX1, explaining some of the observed adjacent spots. However, MX1 seems to have additional post-translational modifications which are not further investigated here.

Phosphorylation of IRF3

Lipopolysaccharide-induced IFN-responsive proteins in THP-1 macrophages, suggest that MyD88-independent TRIF-signaling was induced leading to IRF3 activation by serial C-terminal phosphorylation. Activated IRF3 subsequently dimerizes and translocates into the nucleus.[27] We investigated IRF3 activation by 1-D and 2-D immunoblotting. Consistent with our mRNA expression analysis, total IRF3 expression was stable and insensitive to LPS or CORT treatment at all time points. However, a transient phosphorylation of Ser396 was observed after 1 h of LPS treatment which was blocked by co-treatment with CORT (Fig. 7A). The nuclear translocation of IRF3 was confirmed by 2-D immunoblot of cytosolic and nuclear protein extracts after 48 h of LPS treatment. However, cortisol did not influence this LPS-mediated translocation (Fig. 7B). In order to observe hyperphosphorylation upon LPS treatment, we performed 2-D immunoblots of whole cell lysates, expecting a differential spot pattern over time. IRF3 appeared as four distinct spots suggestive of

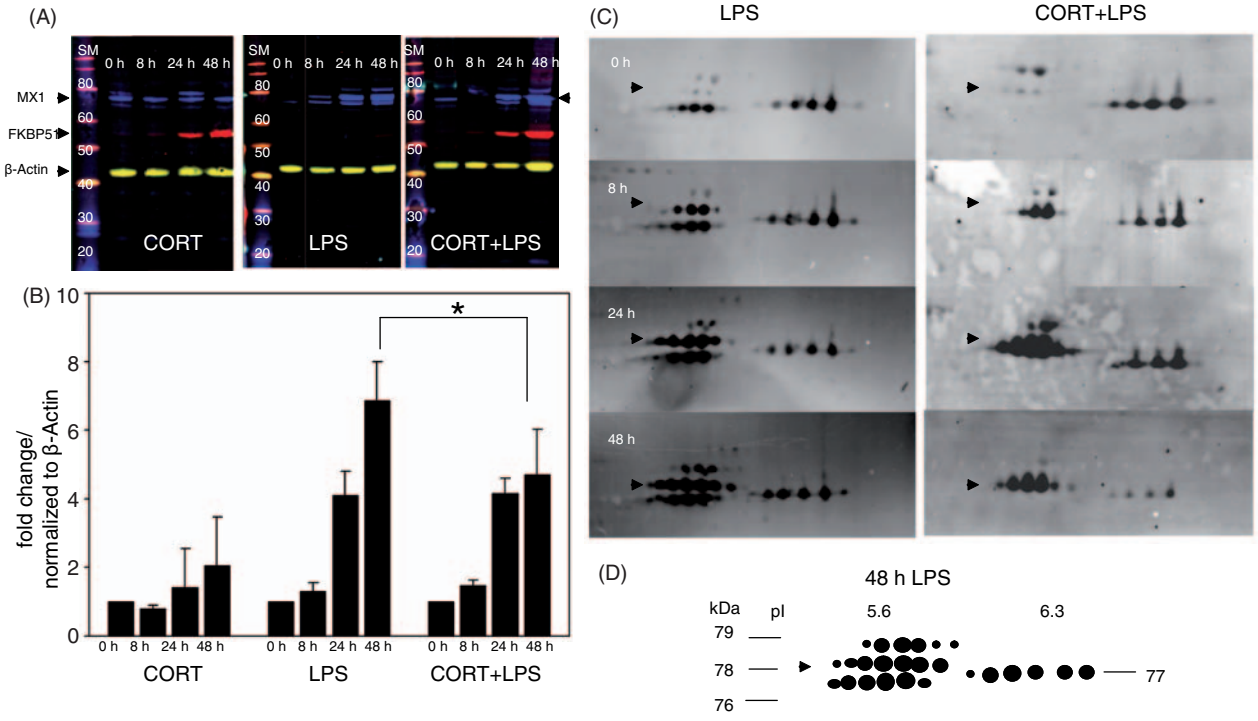

Fig. 6. MX1 and FKBP51 induction. (A) 1-D multiplex immunoblot of FKBP51 and MX1 protein in THP-1 macrophages treated for 8, 24 and 48 h with CORT (10^{-6} M), LPS (1 μg/ml) or a combination of both. β-Actin was stained as a loading control. Bands were visualized with CyDye-labeled secondary Ab: anti-chicken Cy2 (Mx1, blue), anti-mouse Cy3/Cy5 (β -actin, yellow), anti-rabbit Cy5 (FKBP51, red). Aliquots of 10 μg of whole cell lysate was loaded per lane. Three bands are visible for MX1. The second band (annotated with an arrow) corresponds to the major LPS-induced species at 78 kDa. (B) Quantification of MX1 bands on immunoblot. Bars show the relative MX1 induction in relation to β -actin. Data from three independent experiments are presented as mean ± SD. Statistical analysis was performed with SigmaStat v3.1 using two-way ANOVA (Holm–Sidak method). Significant effect of CORT was annotated (*$P < 0.05$). (C) 2-D immunoblots of MX1 protein expression in THP-1 macrophages over 2 days of treatment with LPS (1 μg/ml) or LPS and CORT (10^{-6} M). Arrow indicates the spot group at 78 kDa, corresponding to the annotated band in the 1-D blot (D) Schematic representation of MX1 spot pattern after 48 h LPS.

several post-translational modifications. However, this spot pattern remained largely unchanged after LPS and CORT + LPS treatment (Fig. 7C). Only the unmodified IRF3 spot appeared to be reduced after 1–8 h of LPS and CORT + LPS treatment. The 2-D immunoblot analysis suggests a constitutively modified, probably phosphorylated, IRF3.

We confirmed the LPS-mediated activation of IRF3 by phosphorylation on Ser396 and nuclear translocation. Cortisol only affected the phosphorylation, but not translocation, suggesting a GR-mediated suppression in the nucleus, probably DNA-dependent.

Discussion

Here, we extended our previous proteomics study on THP-1 monocytes[13] to LPS-activated THP-1 macrophages. PMA-induced differentiation of THP-1 cells is a well-established model to study human macrophages[28–34] and differentiation to macrophages was confirmed by typical markers (CD14, CD11b). Nevertheless, PMA treatment may affect additional signaling pathways that are unrelated to macrophage differentiation. The 2 d recovery phase in fresh medium may limit direct effects of PMA. Macrophages are the first line of defense and play a key role bridging innate and adaptive immunity. Co-administration of CORT and LPS mimics the classical inflammatory response coupled with the natural co-activation of the HPA axis correlated with elevated blood CORT levels. Cortisol is thought to modulate the immune response by transrepression of pro-inflammatory genes and by induction of anti-inflammatory genes. Our proteomic data show that, with the exception of HCLS1, an hematopoietic specific adapter molecule with transcriptional activity,[35] all immune response proteins were down-regulated, whereas metabolic proteins were up-regulated. Chaperones, with the exception of FKBP51, were all down-regulated by CORT. This would reduce both antigen-presentation and macrophage activation.[36]

Proteomics combined with bioinformatic pathway profiling identified the LPS-activated IFN type I and

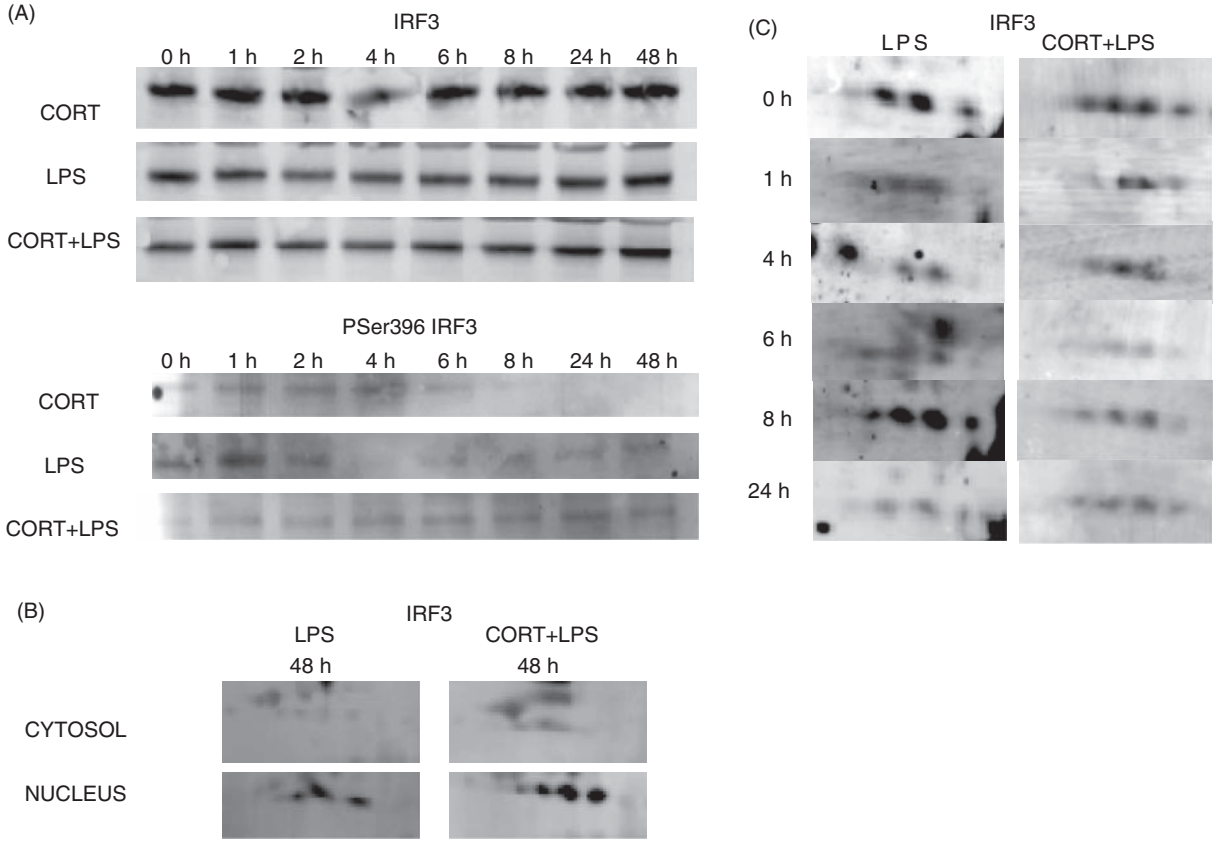

Fig. 7. Induction of the IRF3 pathway. (A) THP-1 macrophages were treated up to 48 h with CORT (10^{-6} M), LPS (1 μg/ml) or CORT + LPS. IRF3 and IRF3 Ser396 phosphorylation were measured by 1-D immunoblot. Whole cell lysate (10 μg) was loaded in each lane. (B) 2-D immunoblot of IRF3 in cytosolic and nuclear protein extracts of THP1 macrophages treated with LPS and CORT + LPS. (C) Representative 2-D immunoblots for IRF3 in THP-1 macrophages which were treated with LPS alone or in combination with CORT for 1, 2, 4, 6, 8, 24, and 48 h. Total protein (30 μg) was separated on a 7-cm IPG strip, pH 4–7.

type II signaling pathways as principal targets of CORT down-regulation. One of the classical type I IFN inducible proteins, the antiviral MX1 protein, was identified as a LPS-inducible CORT-suppressed protein. Its down-regulation by CORT should increase host susceptibility to RNA viruses. Lipopolysaccharide has already been reported to induce MX1,[37–39] although MX1 is not known to have any antibacterial activity. Unexpectedly, MX1 occurred as multiple isoforms on 2-D DIGE gels all of which were induced by LPS and two were suppressed by CORT. Increased sensitivity of 2-D immunoblot revealed a more complex MX1 spot pattern which was affected by CORT. Constitutively expressed MX1 was present in two sets of spots at 76 kDa and 77 kDa separated at the theoretical pI of ± 5.6 and at pI ± 6.3, respectively. These and larger MX1 species (78 kDa and 79 kDa) matching the theoretical pI were induced by LPS. Since for MX1 three phosphotyrosines have been reported, these variants probably correspond to differentially phosphorylated MX1 isoforms, although spot numbers suggest up to six phosphorylation sites. The strong pI shift and changes in molecular mass suggest additional post-translational modifications.

Similarly, the tryptophanyl tRNA synthetase SYWC, a classical type II IFN inducible protein, had multiple isoforms and was induced by LPS and reduced by CORT. In contrast to the full-length protein, none of the three known shorter angiostatic SYWC variants[40,41] were detected in this study; however, a new variant with a lower molecular mass was observed. SYWC is thought to rescue IDO-producing cells from tryptophan starvation,[42] whereas the reduction of SYWC by CORT could slow down translation and eventually inactivate these cells. This may also be a mechanism to release free tryptophan into the micro-environment of the IDO-producing cells, stimulating the production of anti-inflammatory, immunosuppressive tryptophan degradation products. Messenger RNA expression analysis showed that IDO was induced together with SYWC. The LPS-mediated IDO induction has been shown to be mainly IFN-γ-independent.[43] IDO is a potent, CORT-inducible immunosuppressor that helps recruit regulatory T-cells and inhibits T-cell activation and proliferation.[44] In our model, we observed this CORT-mediated IDO induction as well as a CORT-mediated suppression of LPS-induced IDO. This is contrast to IFN-γ-induced IDO, which can be potentiated by CORT.[45]

Amongst the newly identified CORT-modulated proteins was the ubiquitously expressed MGN, a core component of the exon junction complex, responsible for mRNA splicing.[46] MGN has a similar molecular function to HNRPK, that was down-regulated by CORT in both THP-1 monocytes[13] and THP-1 macrophages. It has been shown that the GR specifically affect mRNA processing of steroid-sensitive transcripts by recruiting nuclear receptor co-regulators with splicing activity.[47] Of the HNRP family, HNRPU is known to interact with the GR[48] and to modulate its transcriptional activity.[49] Changes in MGN and HNRPK may modulate steroid-dependent mRNA processing in macrophages and/or monocytes.

Our proteomics data combined with mRNA expression profiling highly suggest that LPS activates the MyD88-independent TRIF signaling pathway leading to IRF3 activation. This was confirmed by immunoblots showing a transient phosphorylation of Ser396, recently identified as a key phosphorylation site for IRF3 activation.[50] This is in agreement with a recent study that showed that both poly:IC and LPS phosphorylate IRF3 on Ser396.[51] We showed that LPS-induced IRF3 phosphorylation on Ser396 is blocked by CORT. According to the current model, cytosolic IRF3 is activated by hyperphosphorylation of the C-terminus, followed by dimerization and translocation to the nucleus.[52] However, nuclear translocation of IRF3 by LPS was not affected by CORT despite the diminished phosphorylation on Ser396. Hyperphosphorylation of IRF3 as described previously[53] was not observed by 2-D immunoblotting. A similar IRF3 2-D spot pattern, comparable to what we observed by immunoblotting, was described in a viral study[54] indicating that those isoforms are not specifically induced by LPS. Recently, a study on direct IRF3 target genes revealed that only a few genes were direct targets, including the proteasome activator 28-β and IFIT3. IRF3 together with NF-κB is known to be responsible for inducing IFN-β and IDO, whereas IRF1 and IRF9 are IRF3-independent.[55]

Glucocorticoid therapy has been used for more than 50 years as a standard treatment of sepsis and related disorders with no clear benefit on mortality except for patients with adrenal insufficiency.[56] It has been shown that sepsis patients often develop critical illness-related corticosteroid insufficiency (CIRCI) which results from either insufficient availability of CORT or CORT tissue insensitivity (despite elevated cortisol level).[57,58] Our study demonstrates that CORT mainly affects the LPS-induced IFN pathway and reflects probably more the response under non-critical conditions. It has been shown by Karaghiosoff and colleagues[59] that IFN-β plays an important role in the onset of endotoxemia and sepsis, and it has been suggested that inhibition of type I IFNs may be of therapeutic interest. The importance of type I IFN mediated signal transduction in sepsis has been shown in several mouse models. Mice lacking parts of the IRF signaling cascade such as TRIF,[3] IRF3,[60] IFN-β,[59] IFNAR[61] or TYK2[59] are resistant to lethal LPS doses. The type II IFN response gene IDO is also implicated in the etiology of sepsis. Blocking of IDO has been shown to protect mice against LPS-induced toxic

shock.[62] IDO, classically induced by IFN-γ, can also be induced by IRF3 and NF-κB downstream of TLR3 signaling.[63] We found IDO strongly induced by LPS, and this induction was efficiently suppressed by CORT. This seems to be beneficial in sepsis, since a higher activity of IDO has been measured in human non-survivors of bacteremia.[64] Our results suggest that exogenous CORT administration (or the concurrent activation of the HPA axis) down-regulates the LPS-induced IRF mediated type I IFN pathway. We hypothesize that the implication of the type I IFN pathway in sepsis proposed here is blocked by CORT treatment. Contrasting clinical observations such as increased IDO levels in patients succumbing to sepsis may reflect CORT insensitivity.

Toll-like receptors, critical for the detection of invading pathogens, link the innate and the adaptive immune system via activation of IRFs. Target genes of IRFs are, for example, IFNs and IFN-inducible genes. IRFs 1, 5 and 8 promote TH1 response, whereas IRF4 promotes TH2-cell responses. IRF1, normally induced by type II IFN, was rapidly induced by LPS and suppressed by CORT. IRF1 induces IL-12 and promotes TH1-cell responses, which would be affected by CORT. A similar regulation pattern was found for IRF9, which mediates in a complex with STAT1/STAT2 as ISGF3 type I IFN responses showing antiviral activity. This is in line with our proteomic data where LPS-induced STAT1 was suppressed by CORT. IRF5, known to be type I IFN inducible, mediates antibacterial activity by the induction of cytokines such as IL-6, IL-12 and TNF. Although we found IFN-β to be LPS-induced, IRF5 showed no response to LPS. Toll-like receptors also affect the HPA axis. Signaling of adrenal gland-expressed TLR2,[65] TLR4[66] and/or TLR9[67] is essential for the secretion of glucocorticoids upon bacterial challenge, whereas CORT has been shown to modulate, for example, TLR2. The immediate induction of an appropriate CORT response is vital, whereas sepsis and septic shock have been associated with impaired HPA axis. Several studies suggest that some TLRs are involved in the etiology of sepsis. It has been shown that TLR1 polymorphisms affect the outcome of sepsis.[68] Also TLR2 plays a key role in sepsis since mortality or reduced resistance in human sepsis has been associated with its reduced expression.[69] We found TLRs 1, 2, 5 and 6 being affected by CORT, all recognizing bacterial-derived ligands. TLR7, the viral ssRNA sensor, was insensitive to CORT, although it was rapidly induced by LPS but suppressed at later time points. The cortisol-mediated induction of TLR2 may enhance antigen-clearance but is in contradiction to the CORT-mediated suppression of TLR1 and TLR6, which heterodimerize with TLR2. Recently, TLR1- and TLR6-independent TLR2 signaling activation has been shown suggesting TLR2 homodimerization.[70] However, TLR2 expression increases in dendritic cells has been associated with a tolerogenic phenotype,[71] which would lead to a reduced pro-inflammatory immune response in sepsis patients.

Conclusions

Lipopolysaccharide treatment greatly influenced the expression of all TLRs, further enhanced or counter regulated by CORT. Our proteomic study shows, in a comprehensive way, the effects of CORT on proteins involved in the immune response, transcription/translation, cytoskeleton and metabolic processes of resting and LPS-activated macrophages. Several new proteins were found to be regulated by CORT and a number of new variants of post-translationally modified proteins such as MX1 were found. Our study also shows that CORT can both up- and down-regulate the same gene, and that this depends on the level of activation or differentiation of the cells. The combined results of proteomics and mRNA expression studies clearly identified the LPS-activated IFN pathway as a complex and prominent target of the immune suppressive activity of CORT. Suppression of the IFN pathway in sepsis may become one of the key therapeutic targets.

Acknowledgements

This study was supported by the Ministry of Culture, Higher Education, and Research, Luxembourg, by the Ministry of Health, Luxembourg, and the Deutsche Forschungsgemeinschaft DFG (International Research Training Group IRTG 1389 'Psychoneuroendocrinology of stress', University of Trier, Germany; University of Leiden, The Netherlands). The authors acknowledge the assistance of the CRP-Gabriel Lippmann. We also thank Hartmut Schächinger and Dirk Hellhammer for their support and initiatives within the DFG-funded IRTG 1389 and the Graduate School of Psychobiology (University of Trier), respectively.

References

1. Rickard AJ, Funder JW, Fuller PJ *et al*. The role of the glucocorticoid receptor in mineralocorticoid/salt-mediated cardiac fibrosis. *Endocrinology* 2006; **147**: 5901–5906.
2. Barish GD, Downes M, Alaynick WA *et al*. A nuclear receptor atlas: macrophage activation. *Mol Endocrinol* 2005; **19**: 2466–2477.
3. Hoebe K, Janssen EM, Kim SO *et al*. Upregulation of costimulatory molecules induced by lipopolysaccharide and double-stranded RNA occurs by Trif-dependent and Trif-independent pathways. *Nat Immunol* 2003; **4**: 1223–1229.

4. Galon J, Franchimont D, Hiroi N *et al*. Gene profiling reveals unknown enhancing and suppressive actions of glucocorticoids on immune cells. *FASEB J* 2002; **16**: 61–71.
5. Ehrchen J, Steinmuller L, Barczyk K *et al*. Glucocorticoids induce differentiation of a specifically activated, anti-inflammatory subtype of human monocytes. *Blood* 2007; **109**: 1265–1274.
6. Fong CC, Zhang Y, Zhang Q *et al*. Dexamethasone protects RAW264.7 macrophages from growth arrest and apoptosis induced by H2O2 through alteration of gene expression patterns and inhibition of nuclear factor-kappa B (NF-kappaB) activity. *Toxicology* 2007; **236**: 16–28.
7. Liu YZ, Dvornyk V, Lu Y *et al*. A novel pathophysiological mechanism for osteoporosis suggested by an *in vivo* gene expression study of circulating monocytes. *J Biol Chem* 2005; **280**: 29011–29016.
8. MacKenzie S, Iliev D, Liarte C *et al*. Transcriptional analysis of LPS-stimulated activation of trout (*Oncorhynchus mykiss*) monocyte/macrophage cells in primary culture treated with cortisol. *Mol Immunol* 2006; **43**: 1340–1348.
9. Ogawa S, Lozach J, Benner C *et al*. Molecular determinants of crosstalk between nuclear receptors and Toll-like receptors. *Cell* 2005; **122**: 707–721.
10. Kang JH, Kim HT, Choi MS *et al*. Proteome analysis of human monocytic THP-1 cells primed with oxidized low-density lipoproteins. *Proteomics* 2006; **6**: 1261–1273.
11. Mouithys-Mickalad A, Deby-Dupont G, Mathy-Hartert M *et al*. Effects of glucocorticoids on the respiratory burst of *Chlamydia*-primed THP-1 cells. *Biochem Biophys Res Commun* 2004; **318**: 941–948.
12. Livak KJ, Schmittgen TD. Analysis of relative gene expression data using real-time quantitative PCR and the 2(-Delta Delta C(T)) Method. *Methods* 2001; **25**: 402–408.
13. Billing AM, Fack F, Renaut J *et al*. Proteomic analysis of the cortisol-mediated stress response in THP-1 monocytes using DIGE technology. *J Mass Spectrom* 2007; **42**: 1433–1444.
14. Honke K, Wada Y. Regulation of vimentin expression and protease-mediated vimentin degradation during differentiation of human monocytic leukemia cells. *Jpn J Cancer Res* 1997; **88**: 484–491.
15. Verhoeckx KC, Bijlsma S, de Groene EM *et al*. A combination of proteomics, principal component analysis and transcriptomics is a powerful tool for the identification of biomarkers for macrophage maturation in the U937 cell line. *Proteomics* 2004; **4**: 1014–1028.
16. Haller O, Staeheli P, Kochs G. Interferon-induced Mx proteins in antiviral host defense. *Biochimie* 2007; **89**: 812–818.
17. Fleckner J, Rasmussen HH, Justesen J. Human interferon gamma potently induces the synthesis of a 55-kDa protein (gamma 2) highly homologous to rabbit peptide chain release factor and bovine tryptophanyl-tRNA synthetase. *Proc Natl Acad Sci USA* 1991; **88**: 11520–11524.
18. Fleckner J, Martensen PM, Tolstrup AB *et al*. Differential regulation of the human, interferon inducible tryptophanyl-tRNA synthetase by various cytokines in cell lines. *Cytokine* 1995; **7**: 70–77.
19. O'Connor JC, Lawson MA, Andre C *et al*. Lipopolysaccharide-induced depressive-like behavior is mediated by indoleamine 2,3-dioxygenase activation in mice. *Mol Psychiatry* 2009; **14**: 511–522.
20. De Miguel F, Lee SO, Onate SA *et al*. Stat3 enhances transactivation of steroid hormone receptors. *Nucl Recept* 2003; **1**: 3.
21. Lou YJ, Pan XR, Jia PM *et al*. IRF-9/STAT2 [corrected] functional interaction drives retinoic acid-induced gene G expression independently of STAT1. *Cancer Res* 2009; **69**: 3673–3680.
22. Huang X, Shen N, Bao C *et al*. Interferon-induced protein IFIT4 is associated with systemic lupus erythematosus and promotes differentiation of monocytes into dendritic cell-like cells. *Arthritis Res Ther* 2008; **10**: R91.
23. Ossendorp F, Fu N, Camps M *et al*. Differential expression regulation of the alpha and beta subunits of the PA28 proteasome activator in mature dendritic cells. *J Immunol* 2005; **174**: 7815–7822.
24. Miettinen M, Sareneva T, Julkunen I *et al*. IFNs activate Toll-like receptor gene expression in viral infections. *Genes Immun* 2001; **2**: 349–355.
25. Zarember KA, Godowski PJ. Tissue expression of human Toll-like receptors and differential regulation of Toll-like receptor mRNAs in leukocytes in response to microbes, their products, and cytokines. *J Immunol* 2002; **168**: 554–561.
26. O'Neill LA, Bowie AG. The family of five: TIR-domain-containing adaptors in Toll-like receptor signalling. *Nat Rev Immunol* 2007; **7**: 353–364.
27. Lin R, Heylbroeck C, Pitha PM *et al*. Virus-dependent phosphorylation of the IRF-3 transcription factor regulates nuclear translocation, transactivation potential, and proteasome-mediated degradation. *Mol Cell Biol* 1998; **18**: 2986–2996.
28. Debbas V, Arai RJ, Ferderbar S *et al*. Regulation of p21Waf1 expression and TNFalpha biosynthesis by glutathione modulators in PMA induced-THP1 differentiation: involvement of JNK and ERK pathways. *Biochem Biophys Res Commun* 2007; **363**: 965–970.
29. Kang SS, Woo SS, Im J *et al*. Human placenta promotes IL-8 expression through activation of JNK/SAPK and transcription factors NF-kappaB and AP-1 in PMA-differentiated THP-1 cells. *Int Immunopharmacol* 2007; **7**: 1488–1495.
30. Kim WJ, Bae EM, Kang YJ *et al*. Glucocorticoid-induced tumour necrosis factor receptor family related protein (GITR) mediates inflammatory activation of macrophages that can destabilize atherosclerotic plaques. *Immunology* 2006; **119**: 421–429.
31. Knowles HJ, Mole DR, Ratcliffe PJ *et al*. Normoxic stabilization of hypoxia-inducible factor-1alpha by modulation of the labile iron pool in differentiating U937 macrophages: effect of natural resistance-associated macrophage protein 1. *Cancer Res* 2006; **66**: 2600–2607.
32. Plattner VE, Ratzinger G, Engleder ET *et al*. Alteration of the glycosylation pattern of monocytic THP-1 cells upon differentiation and its impact on lectin-mediated drug delivery. *Eur J Pharm Biopharm* 2009; **73**: 324–330.
33. Ueki K, Tabeta K, Yoshie H *et al*. Self-heat shock protein 60 induces tumour necrosis factor-alpha in monocyte-derived macrophage: possible role in chronic inflammatory periodontal disease. *Clin Exp Immunol* 2002; **127**: 72–77.
34. Zhou J, Zhu P, Jiang JL *et al*. Involvement of CD147 in overexpression of MMP-2 and MMP-9 and enhancement of invasive potential of PMA-differentiated THP-1. *BMC Cell Biol* 2005; **6**: 25.
35. Kitamura D, Kaneko H, Miyagoe Y *et al*. Isolation and characterization of a novel human gene expressed specifically in the cells of hematopoietic lineage. *Nucleic Acids Res* 1989; **17**: 9367–9379.
36. Tsan MF, Gao B. Heat shock proteins and immune system. *J Leukoc Biol* 2009; **85**: 905–910.
37. Ishii K, Kurita-Taniguchi M, Aoki M *et al*. Gene-inducing program of human dendritic cells in response to BCG cell-wall skeleton (CWS), which reflects adjuvancy required for tumor immunotherapy. *Immunol Lett* 2005; **98**: 280–290.
38. Thomas KE, Galligan CL, Newman RD *et al*. Contribution of interferon-beta to the murine macrophage response to the Toll-like receptor 4 agonist, lipopolysaccharide. *J Biol Chem* 2006; **281**: 31119–31130.

39. Malcolm KC, Worthen GS. Lipopolysaccharide stimulates p38-dependent induction of antiviral genes in neutrophils independently of paracrine factors. *J Biol Chem* 2003; **278**: 15693–15701.
40. Liu J, Shue E, Ewalt KL *et al*. A new gamma-interferon-inducible promoter and splice variants of an anti-angiogenic human tRNA synthetase. *Nucleic Acids Res* 2004; **32**: 719–727.
41. Tolstrup AB, Bejder A, Fleckner J *et al*. Transcriptional regulation of the interferon-gamma-inducible tryptophanyl-tRNA synthetase includes alternative splicing. *J Biol Chem* 1995; **270**: 397–403.
42. Lee GK, Park HJ, Macleod M *et al*. Tryptophan deprivation sensitizes activated T cells to apoptosis prior to cell division. *Immunology* 2002; **107**: 452–460.
43. Fujigaki S, Saito K, Sekikawa K *et al*. Lipopolysaccharide induction of indoleamine 2,3-dioxygenase is mediated dominantly by an IFN-gamma-independent mechanism. *Eur J Immunol* 2001; **31**: 2313–2318.
44. Grohmann U, Volpi C, Fallarino F *et al*. Reverse signaling through GITR ligand enables dexamethasone to activate IDO in allergy. *Nat Med* 2007; **13**: 579–586.
45. Turck J, Oberdorfer C, Vogel T *et al*. Enhancement of antimicrobial effects by glucocorticoids. *Med Microbiol Immunol* 2005; **194**: 47–53.
46. Kataoka N, Diem MD, Kim VN *et al*. Magoh, a human homolog of *Drosophila* mago nashi protein, is a component of the splicing-dependent exon–exon junction complex. *EMBO J* 2001; **20**: 6424–6433.
47. Auboeuf D, Honig A, Berget SM *et al*. Coordinate regulation of transcription and splicing by steroid receptor coregulators. *Science* 2002; **298**: 416–419.
48. Eggert M, Michel J, Schneider S *et al*. The glucocorticoid receptor is associated with the RNA-binding nuclear matrix protein hnRNP U. *J Biol Chem* 1997; **272**: 28471–28478.
49. Eggert H, Schulz M, Fackelmayer FO *et al*. Effects of the heterogeneous nuclear ribonucleoprotein U (hnRNP U/SAF-A) on glucocorticoid-dependent transcription *in vivo*. *J Steroid Biochem Mol Biol* 2001; **78**: 59–65.
50. Chen W, Srinath H, Lam SS *et al*. Contribution of Ser386 and Ser396 to activation of interferon regulatory factor 3. *J Mol Biol* 2008; **379**: 251–260.
51. Clark K, Plater L, Peggie M, Cohen P. Use of the pharmacological inhibitor BX795 to study the regulation and physiological roles of TBK1 and IkappaB kinase epsilon: a distinct upstream kinase mediates Ser-172 phosphorylation and activation. *J Biol Chem* 2009; **284**: 14136–14146.
52. Servant MJ, Grandvaux N, tenOever BR. Identification of the minimal phosphoacceptor site required for in vivo activation of interferon regulatory factor 3 in response to virus and double-stranded RNA. *J Biol Chem* 2003; **278**: 9441–9447.
53. Hiscott J. Triggering the innate antiviral response through IRF-3 activation. *J Biol Chem* 2007; **282**: 15325–15329.
54. Noyce RS, Collins SE, Mossman KL. Differential modification of interferon regulatory factor 3 following virus particle entry. *J Virol* 2009; **83**: 4013–4022.
55. Andersen J, VanScoy S, Cheng TF *et al*. IRF-3-dependent and augmented target genes during viral infection. *Genes Immun* 2008; **9**: 168–175.
56. Annane D, Bellissant E, Bollaert PE *et al*. Corticosteroids in the treatment of severe sepsis and septic shock in adults: a systematic review. *JAMA* 2009; **301**: 2362–2375.
57. Annetta M, Maviglia R, Proietti R *et al*. Use of corticosteroids in critically ill septic patients: a review of mechanisms of adrenal insufficiency in sepsis and treatment. *Curr Drug Targets* 2009; **10**: 887–894.
58. Sprung CL, Annane D, Keh D *et al*. Hydrocortisone therapy for patients with septic shock. *N Engl J Med* 2008; **358**: 111–124.
59. Karaghiosoff M, Steinborn R, Kovarik P *et al*. Central role for type I interferons and Tyk2 in lipopolysaccharide-induced endotoxin shock. *Nat Immunol* 2003; **4**: 471–477.
60. Sakaguchi S, Negishi H, Asagiri M *et al*. Essential role of IRF-3 in lipopolysaccharide-induced interferon-beta gene expression and endotoxin shock. *Biochem Biophys Res Commun* 2003; **306**: 860–866.
61. Hwang SY, Hertzog PJ, Holland KA *et al*. A null mutation in the gene encoding a type I interferon receptor component eliminates antiproliferative and antiviral responses to interferons alpha and beta and alters macrophage responses. *Proc Natl Acad Sci USA* 1995; **92**: 11284–11288.
62. Jung ID, Lee MG, Chang JH *et al*. Blockade of indoleamine 2,3-dioxygenase protects mice against lipopolysaccharide-induced endotoxin shock. *J Immunol* 2009; **182**: 3146–3154.
63. Suh HS, Zhao ML, Rivieccio M *et al*. Astrocyte indoleamine 2,3-dioxygenase is induced by the TLR3 ligand poly(I:C): mechanism of induction and role in antiviral response. *J Virol* 2007; **81**: 9838–9850.
64. Huttunen R, Syrjanen J, Aittoniemi J *et al*. High activity of indoleamine 2,3 dioxygenase enzyme predicts disease severity and case fatality in bacteremic patients. *Shock* 2010; **33**: 149–154.
65. Bornstein SR, Zacharowski P, Schumann RR *et al*. Impaired adrenal stress response in Toll-like receptor 2-deficient mice. *Proc Natl Acad Sci USA* 2004; **101**: 16695–16700.
66. Zacharowski K, Zacharowski PA, Koch A *et al*. Toll-like receptor 4 plays a crucial role in the immune-adrenal response to systemic inflammatory response syndrome. *Proc Natl Acad Sci USA* 2006; **103**: 6392–6397.
67. Tran N, Koch A, Berkels R *et al*. Toll-like receptor 9 expression in murine and human adrenal glands and possible implications during inflammation. *J* Clin Endocrinol Metab 2007; **92**: 2773–2783.
68. Wurfel MM, Gordon AC, Holden TD *et al*. Toll-like receptor 1 polymorphisms affect innate immune responses and outcomes in sepsis. *Am J Respir Crit Care Med* 2008; **178**: 710–720.
69. Schaaf B, Luitjens K, Goldmann T *et al*. Mortality in human sepsis is associated with downregulation of Toll-like receptor 2 and CD14 expression on blood monocytes. *Diagn Pathol* 2009; **4**: 12.
70. Buwitt-Beckmann U, Heine H, Wiesmuller KH *et al*. TLR1- and TLR6-independent recognition of bacterial lipopeptides. *J Biol Chem* 2006; **281**: 9049–9057.
71. Chamorro S, Garcia-Vallejo JJ, Unger WW *et al*. TLR triggering on tolerogenic dendritic cells results in TLR2 up-regulation and a reduced proinflammatory immune program. *J Immunol* 2009; **183**: 2984–2994.